1	Title
2	Bringing Plant Immunity to Light: A Genetically Encoded, Bioluminescent Reporter of
3	Pattern Triggered Immunity in <i>Nicotiana benthamiana</i>
4	Authors
5 6	Anthony G. K. Garcia¹, Adam D. Steinbrenner¹*
7 8	¹ Department of Biology, University of Washington, Seattle WA 98195 U.S.A.
9 10 11	*Corresponding author: A. D. Steinbrenner; E-mail: <u>astein10@uw.edu</u>
12	Keywords: Agrobacterium tumefaciens, bioluminescence, Nicotiana benthamiana,
13	pattern recognition receptor, pattern triggered immunity, receptor-like proteins
14	
15	Funding: National Science Foundation Grant number: IOS-2139986, The Mary Gates
16	Endowment for Students
17	
18	
19	
20	
21	
22	
23	

24

25

26

27

28

29

30

31

32

33

34

35

36

37

38

39

40

41

42

43

Plants rely on innate immune systems to defend against a wide variety of biotic attackers. Key components of innate immunity include cell-surface pattern recognition receptors (PRRs), which recognize pest/pathogen-associated molecular patterns (PAMPs). Unlike other classes of receptors which often have visible cell death immune outputs upon activation, PRRs generally lack rapid methods for assessing function. Here, we describe a genetically encoded bioluminescent reporter of immune activation by heterologously-expressed PRRs in the model organism *Nicotiana benthamiana*. We characterized *N. benthamiana* transcriptome changes in response to *Agrobacterium* tumefaciens (Agrobacterium) and subsequent PAMP treatment to identify PTIassociated marker genes, which were then used to generate promoter-luciferase fusion fungal bioluminescence pathway (FBP) constructs. A reporter construct termed pFBP 2xNbLYS1::LUZ allows for robust detection of PTI activation by heterologously expressed PRRs. Consistent with known PTI signaling pathways, activation by receptorlike protein (RLP) PRRs is dependent on the known adaptor of RLP PRRs, SOBIR1. This system minimizes the amount of labor, reagents, and time needed to assay function of PRRs and displays robust sensitivity at biologically relevant PAMP concentrations, making it ideal for high throughput screens. The tools described in this paper will be powerful for investigations studying PRR function and characterizing the structure-function of plant cell surface receptors.

Introduction

46

45

Plants perceive pests and pathogens through cell surface-localized immune receptors, 47 48 termed pattern recognition receptors (PRRs). Canonically, these transmembrane proteins activate pattern triggered immunity (PTI) in response to conserved pathogen 49 associated molecular patterns (PAMPs) (Boutrot & Zipfel, 2017). PTI consists of a suite 50 51 of defense signaling and outputs including reactive oxygen species (ROS) production, 52 ethylene production, peroxidase upregulation, callose deposition, stomatal 53 modifications, calcium oscillations, and phytohormone production (Aldon et al., 2018; Berens et al., 2017; Broekgaarden et al., 2015; Melotto et al., 2017; Mott et al., 2018; Qi 54 55 et al., 2017; Toyota et al., 2018; Y. Wang et al., 2021). These outputs aid in 56 transcriptional reprogramming to improve plant resistance against attackers (Denoux et 57 al., 2008; Navarro et al., 2004). Understanding immune activation by PRRs is critical for 58 developing novel strategies to improve plant resistance against pests and pathogens. 59 The model organism *Nicotiana benthamiana* represents a significant resource in the field of plant immunity, in part because of robust immune phenotypes conferred by 60 61 transiently expressed intracellular plant immune receptors (Goodin et al., 2008; Buscaill et al., 2021). Agrobacterium-mediated transient transformation of N. benthamiana 62 63 allows for rapid expression of proteins, which is particularly applicable for mutant 64 screening and structure-function analysis. For example, screening cell death as a visual 65 reporter triggered by nucleotide-binding leucine-rich repeat (NLR) activation has allowed investigations of structural features of NLR proteins (Segretin et al., 2014; Steinbrenner 66 67 et al., 2015; Adachi et al., 2019).

Transient transformation of N. benthamiana similarly serves as a powerful tool for 68 69 studying PRRs, but there is currently a lack of robust visual reporters of PRR function in 70 N. benthamiana analogous to cell death. Several cell surface immune receptors activate 71 cell death phenotypes in other species, including leucine-rich repeat receptor-like 72 proteins (LRR-RLPs) such as Arabidopsis thaliana RLP42 and Solanum lycopersicum 73 Ve1, but these LRR-RLPs do not necessarily activate cell death upon heterologous 74 expression in N. benthamiana or can require strong repeated elicitation (de Jonge et al., 2012; Z. Zhang et al., 2013; L. Zhang et al., 2014). Because heterologously expressed 75 76 PRRs do not activate visual markers of PTI in *N. benthamiana*, immune responses 77 mediated by transiently expressed PRRs are instead detected using early markers of 78 PTI defense activation, including PAMP-induced ROS, ethylene, or peroxidase 79 production (Mott et al., 2018; Steinbrenner et al., 2020). However, these assays are 80 laborious or are hampered by the presence of *Agrobacterium* as a background source of PTI activation. 81 82 Reporters utilizing luminescence, fluorescence, or pigmentation have been adapted to 83 study a variety of plant signaling processes (DeBlasio et al., 2010; Furuhata et al., 2020; 84 He et al., 2020). However, no transiently expressed reporters of immune activation in 85 intact N. benthamiana leaves have been described. A high sensitivity luciferase-based system for measuring pattern triggered immunity in protoplasts of *N. benthamiana* was 86 previously reported (Nguyen et al., 2010), but was not tested for heterologously 87 expressed PRRs and required external addition of luciferin. A different system using a 88 89 bioluminescent strain of Agrobacterium expressing the bacterial lux operon allows for monitoring of Agrobacterium during transient transformation and quantification of 90

effector triggered immunity (ETI), but has not yet been applied to PTI (Jutras et al., 2021). *N. benthamiana* lines stably expressing the fluorescent Ca²⁺ indicator GCaMP3 allow for detection of signaling in response to various biotic and abiotic stresses, including signaling activated by transiently expressed receptor-like kinases (DeFalco et al., 2017). However, stable expression of GCaMP3 limits the ability to quickly test different *N. benthamiana* genotypes and mutants lacking components of the signaling pathway. Finally, fluorescent proteins and pigments are simple to measure, but lack the same low background and high sensitivity of luciferase-based assays (Haugwitz et al., 2008; Thorne et al., 2010), which limits the ability to detect the range of responses that may occur in response to an immune elicitor.

To develop a generic PTI reporter, we performed transcriptomic analysis of *N. benthamiana* upon activation of a heterologously expressed PRR and adapted endogenous markers into a luciferase-based system that retains sensitivity but eliminates the need to introduce exogenous substrate. By encoding a metabolic pathway that allows for endogenous production of fungal luciferin alongside the fungal luciferase (*LUZ*) enzyme, the fungal bioluminescence pathway (FBP) system circumvents requirements for external addition of substrate while still remaining sensitive to subtle changes in gene expression (Khakhar et al., 2020; Mitiouchkina et al., 2020). Importantly, the features of the FBP system were well-suited for a reporter system that meets several criteria to be useful for studying plant cell surface immune receptors in a heterologous system: 1) highly sensitive to biologically relevant concentrations of immune elicitors, 2) capable of rapid, low cost, and visual assessment of immune activation, and 3) robust to low numbers of biological replicates and

background immune elicitation by *Agrobacterium*. Therefore, we utilized the FBP system to develop a reporter of immune activation by heterologously expressed cell surface receptors.

Materials and Methods

Plant Materials and Growth Conditions

N. benthamiana plants were transplanted one week after sowing and grown at 20°C under 12-hour light and dark cycles. The seedlings were grown under humidity domes for four weeks, after which the domes were removed, and the plants were grown an additional week before infiltrations. Fully expanded, mature leaves of six-week-old plants were used for all transient expression experiments.

Transcriptomic and qRT-PCR Analysis

For RNA sequencing RNA sequencing analysis, an *N. benthamiana* stable transgenic line expressing *Phaseolus vulgaris* INR (INR-Pv 1-5) (Steinbrenner et al., 2020) was syringe infiltrated with Agrobacterium GV3101 (pMP90) at OD = 0.45 expressing empty vector (EV) pEarleyGate103 (Earley et al., 2006). At 24 hours post infiltration, *Agrobacterium*-treated leaves were further infiltrated with H₂O or 1 μM Inceptin-11 (In11) peptide and harvested after an additional six hours. Total RNA was extracted using Nucleospin Plant RNA kit (#740949.250 Macherey-Nagel). RNA was used to generate Lexogen Quantseq 3' RNA sequencing libraries at Cornell University Institute

of Biotechnology Genomics Facility. 3' reads were mapped to N. benthamiana genome 135 136 v1.0.1 (Sol Genomics Network) using HISAT2 (Kim et al., 2019) with options min-137 intronlen 60--max-intronlen 6000, counts by gene were analyzed using HTSeq-Count 138 (Anders et al., 2015) with options -m intersection-nonempty --nonunique all, and 139 differential expression was analyzed by DESeq2 (Love et al., 2014). 140 For gRT-PCR analysis, N. benthamiana plants were syringe infiltrated with 141 Agrobacterium (OD₆₀₀= 0.45) carrying either p35s::PvINR or pGreenII empty vector. At 142 24 hours after infiltration, tissue was treated with either water or In11 and harvested 143 after 6 hours. Total RNA was extracted using Trizol reagent (#15596018 Thermo Fisher Scientific, USA). cDNA libraries were generated using SuperScript IV Kit (#18090050 144 145 Thermo Fisher Scientific, USA). qRT-PCR reactions were conducted using Applied 146 Biosystems PowerUp SYBR Green Master Mix (#A25742 Thermo Fisher Scientific, 147 USA) and gene specific primer pairs (Supplementary Table S2). Changes in gene 148 expression between water and In11 treatments were calculated using the $\Delta\Delta$ Cq 149 method, using Δ Cq values normalized against N. benthamiana EF1 α (D. Liu et al., 150 2012). Student's t-tests were performed between comparisons of 35s::PvINR and EV

Generation of Reporter Constructs

treated tissue using the ggplot2 package in R (v4.1.2).

151

152

153

154

155

156

Promoter regions of candidate marker genes were amplified from genomic DNA of *N. benthamiana* using primers designed against Niben v1.0.1 (Bombarely et al., 2012) with appended overhangs encoding either Bsal or Bpil restriction enzyme recognition sites (Supplementary Table S2). These primers amplified from the start codon to

approximately 1.5 kb upstream. Promoter regions were then cloned into the Promoter + 157 158 5' untranslated region (UTR) acceptor backbone obtained from the Golden Gate MoClo 159 Plant Toolkit (Engler et al., 2014). Double promoter constructs were constructed by 160 reamplifying the promoter region of interest with unique overhangs and cloning into the 161 Level -1 universal acceptor backbones using the Bsal-HFv2 restriction enzyme 162 (#R3733L New England Biolabs, USA). These parts were then assembled into the 163 same Promoter + 5' UTR acceptor backbone using the Bpil restriction enzyme 164 (#ER1012 Thermo Fisher Scientific, USA). 165 Reporter constructs were generated by first modifying the P307-FBP 6 constitutive 166 autoluminescence construct previously described (Khakhar et al., 2020). P307-FBP 6 167 was a gift from Daniel Voytas (Addgene plasmid # 139697; 168 http://n2t.net/addgene:139697; RRID:Addgene 139697). To simplify the process of 169 cloning new reporter constructs with promoter regions of interest, the CaMV35s 170 promoter originally used to drive LUZ was replaced with an insert encoding a blue-white 171 selectable marker flanked by Bsal recognition sites supplying Promoter + 5' UTR MoClo 172 overhangs (Supplementary Fig. S2A). This allows for simple, one-step assembly 173 reactions. The promoter regions of interest were then cloned into this acceptor plasmid 174 using the Bsal-HFv2 restriction enzyme. A template primer pair for amplification and 175 cloning putative promoter regions directly into the pFBP promoter acceptor construct 176 has been included (Supplementary Table S2). Reporter constructs were transformed by electroporation into Agrobacterium 177 178 tumefaciens GV3101 (pMP90). All sequences were verified by Sanger sequencing.

Agrobacterium-Mediated Transient Transformation and PAMP treatment 179 180 Agrobacterium strains carrying the constructs of interest were cultured in LB media 181 containing kanamycin (50µg/mL), gentamicin (50µg/mL), rifampin (50µg/mL), and 182 tetracycline (10ug/mL) for 24h. 3 mLs of culture were then pelleted and resuspended in 183 infiltration media containing 10mM 2-(N619 morpholino) ethanesulfonic acid (MES) (pH 184 5.6), 10 mM MgCl₂, and 150 µM acetosyringone. For coinfiltrations, separate strains harboring reporter and receptor constructs were combined at a final individual OD₆₀₀ = 185 186 0.3 for a final cumulative OD₆₀₀ = 0.6. After 3 hours of incubation at room temperature 187 (RT), the cell mixture was infiltrated into fully expanded leaves of 6-week-old N. 188 benthamiana plants using a needle-less syringe. 189 To assess induction of luminescence, transformed regions were infiltrated with peptide 48 hours after Agrobacterium infiltration. Six hours after treatment, leaves were 190 191 removed at the petiole and luminescence was immediately imaged using the Azure 192 Imaging System with 8 seconds of exposure. Peptides were obtained from Genscript 193 and diluted to specified concentrations in sterile autoclaved water. 194 **Reactive Oxygen Species Assay** 195 24 hours after infiltration, 4 mm leaf disks were collected from infiltrated tissue and 196 incubated in 150 µL sterile water overnight at room temperature in BRANDplates white 197 96-well plate. Measurement of ROS production was conducted as previously described

(Snoeck et al. 2022). After collection of relative luminescence unit (RLU)

measurements, plots were generated in R using ggplot2. Maximum RLU values were

198

199

calculated and ANOVAs and post-hoc Tukey's t-tests were conducted using the agricolae (v1.3-5) package in R (v4.1.2) and summarized as compact letter displays.

Differing letters represent statistically significant differences (p<0.05) among pairwise comparisons. Figure editing and layouts were completed in Inkscape.

Quantification and Statistical Analysis

Mean gray values of manually defined regions of interest were measured in ImageJ 1.53k. Average signal intensity (ASI) was determined by subtracting the average mean gray value of the untransformed background from the mean gray values of the regions of interest. Negative ASI indicates lower mean gray value than background. One-way ANOVAs and post-hoc Tukey's t-tests were conducted using the agricolae (v1.3-5) package in R (v4.1.2) and summarized as compact letter displays. Differing letters represent statistically significant differences (p<0.05) among pairwise comparisons. Figure editing and layouts were completed in Inkscape.

Phylogenetic Analysis

Using the annotated coding sequence of *Niben101Scf06684g03003.1*, a BLASTN search was conducted against the *Vigna unguiculata* (v1.2), *Phaseolus vulgaris* (v2.1), and *Arabidopsis thaliana* (TAIR10) genomes (predicted cDNA sequences). *Arabidopsis thaliana* was included to identify potential characterized homologs, and the two legume species were included as representative legume species that natively encode INR. After aligning the top 70 hits, a maximum likelihood phylogenetic tree was generated using FastTree. A subset of this tree was then selected and realigned as translated amino

acid sequences using MAFFT (Katoh et al., 2019; Kuraku et al., 2013). A maximum likelihood tree was subsequently generated on the CIPRES web portal using RAXML-HPC2 on XSEDE (v8.2.12) (Miller et al., 2010; Stamatakis, 2014) with the automatic protein model assignment algorithm using maximum likelihood criterion and 100 bootstrap replicates. The resulting phylogeny was rooted and visualized using MEGA11 and edited in Inkscape.

Results

Differentially Expressed Genes in Response to *Agrobacterium* and PTI activation

Heterologous expression of PRRs in *N. benthamiana* allows for activation of PTI in response to cognate PAMPs, but transient expression requires introduction of *Agrobacterium*, a potentially independent source of PAMPs and activator of PTI responses. To characterize the transcriptional landscape of PTI induced by both *Agrobacterium* and individual PAMP treatment, we conducted transcriptomic analysis in plants stably expressing the *P. vulgaris* Inceptin Receptor (PvINR), an LRR-RLP which recognizes the peptide elicitor inceptin11 (In11) (Steinbrenner et al., 2020). Plants were infiltrated with *Agrobacterium* to mimic conditions during *Agrobacterium*-mediated transient transformation. After 24 hours, the *Agrobacterium*-infiltrated leaves were subsequently treated with water or In11 to induce immune signaling (Supplementary Fig. S1, "AH" or "AI"). Additionally, leaves previously mock infiltrated were infiltrated with water to account for effects of wounding during infiltration (Supplementary Fig. S1, "H").

Tissue was collected after 6 hours, and RNA sequencing was subsequently conducted 243 244 to identify differentially expressed genes (DEGs) under each pair of conditions. 245 Compared to leaf tissue not previously infiltrated, infiltration with Agrobacterium affected expression of hundreds of genes (Fig. 1A, comparisons "AH vs H" and "AI vs H", 246 247 Supplementary Table S1). A total of 1425 upregulated and 938 downregulated genes 248 were significantly altered by Agrobacterium infiltration. The majority of DEGs were 249 observed in both In11 and water treated tissue. 250 To identify useful markers of PTI activation in the context of *Agrobacterium*, we next 251 compared gene expression in Agrobacterium-infiltrated leaf tissue in the presence or 252 absence of In11 peptide (AI vs AH). Only one gene was significantly differentially 253 expressed (Supplementary Table S1, column "adj. p"). Since In11 treatment previously activated measurable early immune phenotypes (Steinbrenner et al., 2020), namely 254 255 induced ROS and ethylene production, in identical experimental conditions, we 256 reasoned that transcriptional changes at this timepoint may occur below the threshold 257 for statistical significance. We therefore performed a separate analysis filtering for genes with p<0.05 differential expression by standard Wald test but without correction 258 259 for multiple comparisons (Supplementary Fig. S1B, Supplementary Table S1, column "p-value"). With this relaxed threshold, 91 genes were characterized as upregulated by 260 261 the addition of In11 (Supplementary Fig. S1). Interestingly, In11-upregulated genes 262 overlapped with both Agrobacterium-upregulated (Supplementary Fig. S1B) and downregulated genes (Supplementary Fig. S1C), suggesting complex regulation of 263 264 specific N. benthamiana PTI outputs.

We further filtered candidate PTI marker genes based on broad responsiveness to both Agrobacterium and In11. Nine genes showed higher Agrobacterium or In11 induced expression in all three comparisons (Fig. 1C, Supplementary Fig. S1B), suggesting a large dynamic range of gene expression able to be activated by both Agrobacterium PAMPs and by the addition of the separate individual PAMP, In11. To determine more confidently which of these genes are induced by In11 treatment, we conducted qRT-PCR analysis probing differences in expression of each of the candidate marker genes six hours after water and In11 treatment. We found that four genes showed significant induction after treatment with In11 in tissue transiently expressing PvINR, but not in tissue infiltrated with an empty vector strain: Niben101Scf08566g08014, Niben101Scf04592g00020, Niben101Scf06684g03003, Niben101Scf04652g00027 (Fig. 2). We conclude that these four genes serve as markers of INR-mediated responses to In11 in *Nicotiana benthamiana* after transient PRR expression. In summary, while the transcriptional effects of an additional PAMP, In11, 24 hours after Agrobacterium infiltration are subtle, candidate genes were observed with Agrobacterium and PAMPinducible behavior consistent with broadly responsive marker genes.

265

266

267

268

269

270

271

272

273

274

275

276

277

278

279

280

281

282

283

284

285

286

An FBP Luminescence Reporter to Quantify Innate Immune Activation by PTI

To test whether the promoter regions of these genes could function in In11-inducible reporters, we generated promoter fusion constructs with promoter regions of the endogenous *N. benthamiana* marker genes driving expression of the fungal luciferase (LUZ). Original FBP constructs contain five genes of the pathway for both LUZ and substrate biosynthesis enzymes (Khakhar et al., 2020). We first generated an adaptable

luminescence between water and In11 treatment, while the p2xLYS1::LUZ double copy

309

construct did show a significant difference between the water and In11 treatments (Fig. 310 311 3A). We therefore elected to proceed using the p2xLYS1::LUZ FBP construct as a 312 reporter for all subsequent experiments. 313 Different assays for immune receptor function show varying degrees of sensitivity to low 314 elicitor concentrations (Mott et al., 2018). To determine the sensitivity of the FBP 315 reporter assay to In11 treatment, we coexpressed the p2xLYS1::LUZ reporter and 316 p35s::PvINR and conducted a dose-response experiment using increasing 317 concentrations of In11. We observed statistically significant differences in luminescence 318 between water and In11 treatments above 500 pM (Fig. 3B). This falls within the range of reported In11 concentrations that are present in the oral secretions of caterpillars 319 320 during herbivory (Schmelz et al., 2006), and represents a potentially higher sensitivity 321 than that of a ROS assay (Supplementary Fig S6). As a result, the p2xLYS1::LUZ is a 322 robust reporter of immune activation by biologically relevant elicitor concentrations. 323 Besides INR, other heterologously expressed PRRs are capable of conferring PTI 324 immune signaling in N. benthamiana (Albert et al., 2015; Steinbrenner et al., 2020; L. 325 Zhang et al., 2021). Furthermore, flg22 treatment induces expression of the A. thaliana 326 LYS1 homolog (X. Liu et al., 2014). To test whether the p2xLYS1::LUZ construct serves as a reporter of PRR activity more broadly, we also tested reporter inducibility by two 327 328 cell surface PRRs from A. thaliana: EFR and RLP23. We observed background 329 induction of luminescence in leaf tissue expressing EFR when treated with elf18 (Fig. 4C, Supplementary Fig. S7). This is potentially due to background induction of EFR by 330 331 Agrobacterium, an EFR-specific effect further supported by lack of background

luminescence in tissue expressing AtFLS2 (Supplementary Fig. S8). elf18 nonetheless 332 333 robustly induces luminescence relative to mock treatment. We also observed induction 334 of luminescence in leaf tissue expressing RLP23 when treated with nlp20 (Fig. 4D). 335 Importantly, induction of luminescence is only observed in regions of interest where the 336 cognate receptor-elicitor pair is present. Together, these data support the utility of the 337 p2xLYS1::LUZ construct as a robust reporter of specific PRR-elicitor interactions. SOBIR1 is necessary for INR-mediated Induction of Bioluminescence by Inceptin 338 339 Characterized LRR-RLPs are known to require the adaptor receptor-kinase 340 SUPPRESSOR OF BIR1-1 (SOBIR1) to initiate downstream signaling (Liebrand et al., 341 2013; Albert et al., 2015). Although SOBIR1 has been shown to associate with INR in 342 Nicotiana benthamiana, it is not yet known if SOBIR1 is necessary for immune signaling 343 by PvINR (Steinbrenner et al., 2020). To determine whether PvINR requires SOBIR1 344 and whether the p2xLYS1::LUZ reflects downstream immune signaling pathways, we conducted reporter assays in N. benthamiana sobir1 knockout plants, which previously 345 346 showed compromised function of the tomato LRR-RLP Cf4 (Huang et al., 2021). 347 Induction of luminescence by In11 treatment is absent in sobir1 mutant plants and 348 restored when either A. thaliana SOBIR1 or P. vulgaris SOBIR1 are coexpressed with PvINR. (Fig. 5). Thus, reporter activation is subject to similar requirements for LRR-349 350 RLP function as well-characterized PTI responses. This suggests that the 351 p2xLYS1::LUZ construct serves as a useful tool not only for studying receptor-elicitor interactions but also downstream interactions important for immune activation and 352 353 signaling.

355

Discussion

356

357

358

359

360

361

362

363

364

365

366

367

368

369

370

371

372

373

374

375

We describe here a genetically encoded reporter responsive to heterologously expressed PRRs in *N. benthamiana*. The *p2xLYS1::LUZ* reporter demonstrates robust PAMP sensitivity and does not require addition of exogenous enzyme substrate. Therefore, this reporter assay may be a useful tool for assessing immune activation by a number of diverse PRRs, including both receptor-like kinases and receptor-like proteins. To develop this reporter, we first characterized the transcriptional modifications that occur in response to both Agrobacterium and elicitor perception by a heterologously expressed LRR-RLP. LRR-RLPs warrant further structural and functional characterization, as they constitute a key class of PRRs involved in activating plant innate immune responses (Jamieson et al., 2018; Albert et al., 2020; Steinbrenner, 2020). LRR-RLPs also include the first known receptor-ligand pair involved in defense against a chewing herbivore (Steinbrenner et al., 2020). However, the specific molecular interactions required for immune signaling by LRR-RLPs in plants remain only partially understood, in part because no solved crystal structures of LRR-RLPs have been reported. Although characterized LRR-RLPs require SUPPRESSOR OF BIR1-1 (SOBIR1) and SOMATIC EMBRYOGENESIS RECEPTOR KINASES (SERKS) to activate immune signaling, the mechanisms underlying ligand binding and coreceptor

association are unclear (van der Burgh et al., 2019). As a result, we tailored our reporter

system toward heterologously expressed LRR-RLPs to aid in gathering deeper insights into this important and incompletely understood group of plant cell surface immune receptors. However, we also observed induction of luminescence in response to the bacterial elicitor elf18 in tissue expressing *A. thaliana* EFR, a receptor-like kinase (RLK) (Zipfel et al., 2006). As a result, this reporter could be useful for studying RLK signaling. Additionally, recent studies describing the overlap between PTI and ETI signaling suggest common signaling components (Ngou et al., 2021; Pruitt et al., 2021). As a result, there is a possibility this reporter could serve to study intracellular immune receptors and may be particularly useful when these receptors do not produce hypersensitive responses.

Unsurprisingly, our transcriptomic analysis revealed that *Agrobacterium* treatment alone resulted in large changes in gene expression. This demonstrates that *Agrobacterium* strongly induces innate immunity in *N. benthamiana*, likely through recognition of *Agrobacterium* PAMPs, resulting in large-scale transcriptional changes. Therefore, it is important to consider the role of *Agrobacterium* PAMPs in activating immunity. Interestingly, many genes that showed upregulation in response to In11 treatment were genes that were downregulated by *Agrobacterium* (Fig S1B-C). While likely due to timescales of *Agrobacterium* inoculation (24 hours post infiltration) versus In11 treatment (6 hours post infiltration), it is also possible that perception of *Agrobacterium* PAMPs by *N. benthamiana* is antagonized by simultaneous activation of immunity by the herbivore-associated In11 elicitor, a potential result of signaling conflict between SA and JA signaling (Li et al., 2019). *Agrobacterium* may activate biotroph-related immunity, whereas INR may activate necrotroph-related immunity through pathways

downstream of SOBIR1. Because of the complex nature of these factors, we selected genes that showed upregulation in response to *Agrobacterium* that was further amplified by In11 treatment to identify a generic marker of immune activation by specific elicitor

402 receptor interactions.

399

400

401

403

404

405

406

407

408

409

410

411

412

413

414

415

416

417

418

419

420

Although we identified four marker candidates, only one showed induction of luminescence in response to elicitor treatment (Fig. 3). We were either unable to clone the respective promoter region (Niben101Scf04592q00020, Niben101Scf04652q00027) or observed no luminescence in response to In11 treatment compared to water treatment (Niben101Scf08566q08014) (Supplementary Fig. S2). Although protocols exist to amplify difficult templates such as AT or GC-rich sequences (Dhatterwal et al., 2017; Sahdev et al., 2007), the complex nature of the N. benthamiana genome poses technical challenges in amplifying already evasive promoter regions (Bombarely et al., 2012). Furthermore, it is possible that promoter terminator incompatibility occurred between candidate promoter regions resulting in silencing of LUZ (P.-H. Wang et al., 2020). Finally, it is possible that we failed to include the necessary cis-regulatory elements of the promoter region, as we decided on a somewhat arbitrary cutoff of 1.5 kb preceding the start codon of the gene. Trans-regulatory elements may also be necessary to mediate observed changes in gene expression in response to In11 treatment. As a result, improved understanding of plant transcriptional regulatory elements will facilitate efforts to identify and utilize additional highly responsive promoters under a variety of biotic stress conditions as tools to study plant immune responses.

The pFBP promoter acceptor construct is now publicly available to screen other candidate promoters through simple MoClo ligation of a promoter of interest. However, several considerations should be taken regarding the use of the FBP reporter. Unlike firefly luciferase, which is known to have a short half-life in the presence of luciferin (Van Leeuwen et al., 2000), it is suggested that the stability of fungal luciferase is more suitable for measuring changes over hours, limiting its utility on finer time scales (Khakhar et al., 2020). Induction of luminescence should as a result be viewed as a cumulative representation of reporter activity, rather than instantaneous measure of gene expression. Furthermore, production of fungal luciferin depends on availability of caffeic acid, causing luciferin availability to not be completely uniform across all plant tissues, and sustained periods of fungal luciferase activity to possibly deplete luciferin stores. Although these limitations remain largely negligible for the purpose of assessing specific receptor-elicitor interactions, they should be considered in situations where temporal and spatial aspects are of importance. It should be noted that the FBP construct designed by Khakhar et al includes caffeylpyruvate hydrolase (CPH), which converts the product of the luciferase-luciferin assay, caffeylpyruvic acid, back to caffeic acid. This allows for recycling of luciferin that prolongs bioluminescence production, circumventing one potential issue for prolonged measures. Because this reporter assay was used to measure relatively short time-scale processes, it is unlikely to be critical for function of the assay. A final consideration regarding caffeic acid dynamics relates to the role of caffeic acid

421

422

423

424

425

426

427

428

429

430

431

432

433

434

435

436

437

438

439

440

441

442

443

as an important compound mediating plant stress resistance. Efforts to utilize caffeic acid to aid in resistance to abiotic stresses demonstrate important effects on enhancing resistance (Klein et al. 2013, Wan et al. 2015, Mehmood et al. 2021). During plant immunity, caffeic acid can similarly play important roles. Induction of caffeic acid in Nicotiana tabacum during infection by Ralstonia solanacearum aids in plant defense (Li et al. 2021), and caffeic acid accumulation has been widely shown to enhance resistance to pathogens by increasing lignification of plant tissue (Riaz et al. 2019). In our reporter system, induction of luminescence upon activation of immunity was only observed with reporter fusion constructs harboring the NbLYS1 homolog promoter region, and not with the constitutive *CaMV35s* promoter region. This supports the conclusion that under this system, the reaction catalyzed by fungal luciferase represents the rate limiting step for production of luminescence, rather than changing caffeic acid dynamics. Although we did not further disentangle caffeic acid induction during pattern triggered immunity, it presents an interesting avenue in the field of plant secondary metabolites. This reporter system represents a potentially high-throughput and sensitive reporter for assessing immune activation by heterologously expressed PRRs in N. benthamiana. Although other systems retain power by being more sensitive to subtle immune phenotypes and usefulness in characterizing endogenous immune signaling processes in non-model organisms, the sensitivity, robustness, and ease of the FBP reporter system make it useful for understanding cell surface receptor function in N. benthamiana. As a result, this reporter represents a potentially valuable addition to the plant immune biology toolkit, especially for large scale studies aimed at illuminating the

structure and function of cell surface immune receptors from diverse species.

444

445

446

447

448

449

450

451

452

453

454

455

456

457

458

459

460

461

462

463

464

465

Acknowledgements 466 We thank members of the Steinbrenner, Imaizumi and Nemhauser labs at UW Biology 467 468 for helpful discussion and comments. This work was supported by NSF grant IOS-469 2139986 and the UW Mary Gates Endowment for Students. 470 **Author Contributions** 471 472 A.D.S. conducted the transcriptomic analysis. A.G.K.G. conducted subsequent 473 experiments. A.D.S. and A.G.K.G wrote the manuscript. 474 **Materials Availability** 475 Transcriptomic data are available in NCBI SRA (BioProject number PRJNA902803). 476 The pFBP promoter acceptor and pFBP 2xNbLYS1::LUZ constructs are available at Addgene (plasmid numbers 189920 and 189918 respectively). 477 References 478 479 480 Adachi, H., Contreras, M. P., Harant, A., Wu, C., Derevnina, L., Sakai, T., Duggan, C., 481 Moratto, E., Bozkurt, T. O., Magbool, A., Win, J., & Kamoun, S. (2019). An N-482 483 terminal motif in NLR immune receptors is functionally conserved across distantly related plant species. ELife, 8, e49956. https://doi.org/10.7554/eLife.49956 484 Albert, I., Böhm, H., Albert, M., Feiler, C. E., Imkampe, J., Wallmeroth, N., Brancato, C., 485 486 Raaymakers, T. M., Oome, S., Zhang, H., Krol, E., Grefen, C., Gust, A. A., Chai,

J., Hedrich, R., Van den Ackerveken, G., & Nürnberger, T. (2015). An RLP23-487 488 SOBIR1-BAK1 complex mediates NLP-triggered immunity. *Nature Plants*, 1(10), 489 1–9. https://doi.org/10.1038/nplants.2015.140 Albert, I., Hua, C., Nürnberger, T., Pruitt, R. N., & Zhang, L. (2020). Surface Sensor 490 491 Systems in Plant Immunity. *Plant Physiology*, 182(4), 1582–1596. 492 https://doi.org/10.1104/pp.19.01299 493 Aldon, D., Mbengue, M., Mazars, C., & Galaud, J.-P. (2018). Calcium Signalling in Plant 494 Biotic Interactions. International Journal of Molecular Sciences, 19(3), 665. 495 https://doi.org/10.3390/ijms19030665 496 Anders, S., Pyl, P. T., & Huber, W. (2015). HTSeq—A Python framework to work with 497 high-throughput sequencing data. Bioinformatics, 31(2), 166–169. 498 https://doi.org/10.1093/bioinformatics/btu638 499 Berens, M. L., Berry, H. M., Mine, A., Argueso, C. T., & Tsuda, K. (2017). Evolution of 500 Hormone Signaling Networks in Plant Defense. Annual Review of 501 Phytopathology, 55(1), 401–425. https://doi.org/10.1146/annurev-phyto-080516-502 035544 503 Bombarely, A., Rosli, H. G., Vrebalov, J., Moffett, P., Mueller, L. A., & Martin, G. B. 504 (2012). A Draft Genome Sequence of Nicotiana benthamiana to Enhance 505 Molecular Plant-Microbe Biology Research. *Molecular Plant-Microbe Interactions*, 25(12), 1523-1530. https://doi.org/10.1094/MPMI-06-12-0148-TA 506 507 Boutrot, F., & Zipfel, C. (2017). Function, Discovery, and Exploitation of Plant Pattern 508 Recognition Receptors for Broad-Spectrum Disease Resistance. Annual Review 509 of Phytopathology, 55, 257–286, https://doi.org/10.1146/annurey-phyto-080614-

510	120106
511	Broekgaarden, C., Caarls, L., Vos, I. A., Pieterse, C. M. J., & Van Wees, S. C. M.
512	(2015). Ethylene: Traffic Controller on Hormonal Crossroads to Defense. Plant
513	Physiology, 169(4), 2371–2379. https://doi.org/10.1104/pp.15.01020
514	Buscaill, P., Sanguankiattichai, N., Lee, Y. J., Kourelis, J., Preston, G., & van der Hoorn,
515	R. A. L. (2021). Agromonas: A rapid disease assay for Pseudomonas syringae
516	growth in agroinfiltrated leaves. The Plant Journal, 105(3), 831–840.
517	https://doi.org/10.1111/tpj.15056
518	de Jonge, R., Peter van Esse, H., Maruthachalam, K., Bolton, M. D., Santhanam, P.,
519	Saber, M. K., Zhang, Z., Usami, T., Lievens, B., Subbarao, K. V., & Thomma, B.
520	P. H. J. (2012). Tomato immune receptor Ve1 recognizes effector of multiple
521	fungal pathogens uncovered by genome and RNA sequencing. Proceedings of
522	the National Academy of Sciences, 109(13), 5110–5115.
523	https://doi.org/10.1073/pnas.1119623109
524	DeBlasio, S. L., Sylvester, A. W., & Jackson, D. (2010). Illuminating plant biology: Using
525	fluorescent proteins for high-throughput analysis of protein localization and
526	function in plants. Briefings in Functional Genomics, 9(2), 129–138.
527	https://doi.org/10.1093/bfgp/elp060
528	DeFalco, T. A., Toyota, M., Phan, V., Karia, P., Moeder, W., Gilroy, S., & Yoshioka, K.
529	(2017). Using GCaMP3 to Study Ca2+ Signaling in Nicotiana Species. Plant and
530	Cell Physiology, 58(7), 1173-1184. https://doi.org/10.1093/pcp/pcx053
531	Denoux, C., Galletti, R., Mammarella, N., Gopalan, S., Werck, D., De Lorenzo, G.,
532	Ferrari, S., Ausubel, F. M., & Dewdney, J. (2008). Activation of Defense

Response Pathways by OGs and Flg22 Elicitors in Arabidopsis Seedlings. 533 534 Molecular Plant, 1(3), 423–445. https://doi.org/10.1093/mp/ssn019 Dhatterwal, P., Mehrotra, S., & Mehrotra, R. (2017). Optimization of PCR conditions for 535 536 amplifying an AT-rich amino acid transporter promoter sequence with high 537 number of tandem repeats from Arabidopsis thaliana. BMC Research Notes, 10, 538 638. https://doi.org/10.1186/s13104-017-2982-1 539 Earley, K. W., Haag, J. R., Pontes, O., Opper, K., Juehne, T., Song, K., & Pikaard, C. S. 540 (2006). Gateway-compatible vectors for plant functional genomics and 541 proteomics. The Plant Journal, 45(4), 616–629. https://doi.org/10.1111/j.1365-542 313X.2005.02617.x 543 Engler, C., Youles, M., Gruetzner, R., Ehnert, T.-M., Werner, S., Jones, J. D. G., Patron, 544 N. J., & Marillonnet, S. (2014). A Golden Gate Modular Cloning Toolbox for Plants. ACS Synthetic Biology, 3(11), 839–843. 545 546 https://doi.org/10.1021/sb4001504 547 Furuhata, Y., Sakai, A., Murakami, T., Nagasaki, A., & Kato, Y. (2020). Bioluminescent 548 imaging of Arabidopsis thaliana using an enhanced Nano-lantern luminescence reporter system. *PLoS ONE*, 15(1), e0227477. 549 550 https://doi.org/10.1371/journal.pone.0227477 551 Goodin, M. M., Zaitlin, D., Naidu, R. A., & Lommel, S. A. (2008). Nicotiana benthamiana: Its History and Future as a Model for Plant-Pathogen Interactions. 552 553 Molecular Plant-Microbe Interactions, 21(8), 1015–1026. https://doi.org/10.1094/MPMI-21-8-1015 554 555 Haugwitz, M., Nourzaie, O., Garachtchenko, T., Hu, L., Gandlur, S., Olsen, C., Farmer,

	26
556	A., Chaga, G., & Sagawa, H. (2008). Multiplexing Bioluminescent and
557	Fluorescent Reporters to Monitor Live Cells. Current Chemical Genomics, 1, 11-
558	19. https://doi.org/10.2174/1875397300801010011
559	He, Y., Zhang, T., Sun, H., Zhan, H., & Zhao, Y. (2020). A reporter for noninvasively
560	monitoring gene expression and plant transformation. Horticulture Research,
561	7(1), 1–6. https://doi.org/10.1038/s41438-020-00390-1
562	Huang, W. R. H., Schol, C., Villanueva, S. L., Heidstra, R., & Joosten, M. H. A. J.
563	(2021). Knocking out SOBIR1 in Nicotiana benthamiana abolishes functionality of
564	transgenic receptor-like protein Cf-4. Plant Physiology, 185(2), 290–294.
565	https://doi.org/10.1093/plphys/kiaa047
566	Jamieson, P. A., Shan, L., & He, P. (2018). Plant cell surface molecular cypher:
567	Receptor-like proteins and their roles in immunity and development. Plant
568	Science, 274, 242–251. https://doi.org/10.1016/j.plantsci.2018.05.030
569	Jutras, P. V., Soldan, R., Dodds, I., Schuster, M., Preston, G. M., & van der Hoorn, R.
570	A. L. (2021). AgroLux: Bioluminescent Agrobacterium to improve molecular
571	pharming and study plant immunity. The Plant Journal, 108(2), 600–612.
572	https://doi.org/10.1111/tpj.15454
573	Katoh, K., Rozewicki, J., & Yamada, K. D. (2019). MAFFT online service: Multiple
574	sequence alignment, interactive sequence choice and visualization. Briefings in
575	Bioinformatics, 20(4), 1160–1166. https://doi.org/10.1093/bib/bbx108

Kay, R., Chan, A., Daly, M., & McPherson, J. (1987). Duplication of CaMV 35S

236(4806), 1299–1302.

Promoter Sequences Creates a Strong Enhancer for Plant Genes. Science,

576

577

578

579	Khakhar, A., Starker, C. G., Chamness, J. C., Lee, N., Stokke, S., Wang, C., Swanson,
580	R., Rizvi, F., Imaizumi, T., & Voytas, D. F. (2020). Building customizable auto-
581	luminescent luciferase-based reporters in plants. ELife, 9, e52786.
582	https://doi.org/10.7554/eLife.52786
583	Kim, D., Paggi, J. M., Park, C., Bennett, C., & Salzberg, S. L. (2019). Graph-based
584	genome alignment and genotyping with HISAT2 and HISAT-genotype. Nature
585	Biotechnology 37(8), 907–915. https://doi.org/10.1038/s41587-019-0201-4
586	Kuraku, S., Zmasek, C. M., Nishimura, O., & Katoh, K. (2013). ALeaves facilitates on-
587	demand exploration of metazoan gene family trees on MAFFT sequence
588	alignment server with enhanced interactivity. Nucleic Acids Research, 41(W1),
589	W22–W28. https://doi.org/10.1093/nar/gkt389
590	Li, N., Han, X., Feng, D., Yuan, D., & Huang, LJ. (2019). Signaling Crosstalk between
591	Salicylic Acid and Ethylene/Jasmonate in Plant Defense: Do We Understand
592	What They Are Whispering? International Journal of Molecular Sciences, 20(3),
593	671. https://doi.org/10.3390/ijms20030671
594	Liebrand, T. W. H., van den Berg, G. C. M., Zhang, Z., Smit, P., Cordewener, J. H. G.,
595	America, A. H. P., Sklenar, J., Jones, A. M. E., Tameling, W. I. L., Robatzek, S.,
596	Thomma, B. P. H. J., & Joosten, M. H. A. J. (2013). Receptor-like kinase
597	SOBIR1/EVR interacts with receptor-like proteins in plant immunity against
598	fungal infection. Proceedings of the National Academy of Sciences, 110(24),
599	10010–10015. https://doi.org/10.1073/pnas.1220015110
600	Liu, D., Shi, L., Han, C., Yu, J., Li, D., & Zhang, Y. (2012). Validation of Reference
601	Genes for Gene Expression Studies in Virus-Infected Nicotiana benthamiana

Using Quantitative Real-Time PCR. PLoS ONE, 7(9), e46451. 602 603 https://doi.org/10.1371/journal.pone.0046451 Liu, X., Grabherr, H. M., Willmann, R., Kolb, D., Brunner, F., Bertsche, U., Kühner, D., 604 Franz-Wachtel, M., Amin, B., Felix, G., Ongena, M., Nürnberger, T., & Gust, A. A. 605 606 (2014). Host-induced bacterial cell wall decomposition mediates pattern-triggered 607 immunity in Arabidopsis. *ELife*, 3, e01990. https://doi.org/10.7554/eLife.01990 608 Love, M. I., Huber, W., & Anders, S. (2014). Moderated estimation of fold change and 609 dispersion for RNA-seg data with DESeg2. Genome Biology, 15(12), 550. 610 https://doi.org/10.1186/s13059-014-0550-8 Melotto, M., Zhang, L., Oblessuc, P. R., & He, S. Y. (2017). Stomatal Defense a Decade 611 612 Later. *Plant Physiology*, 174(2), 561–571. https://doi.org/10.1104/pp.16.01853 613 Miller, M. A., Pfeiffer, W., & Schwartz, T. (2010). Creating the CIPRES Science 614 Gateway for inference of large phylogenetic trees. *Proceedings of the Gateway* Computing Environments Workshop (GCE), 1–8. 615 616 https://doi.org/10.1109/GCE.2010.5676129 617 Mitiouchkina, T., Mishin, A. S., Somermeyer, L. G., Markina, N. M., Chepurnyh, T. V., Guglya, E. B., Karataeva, T. A., Palkina, K. A., Shakhova, E. S., Fakhranurova, 618 619 L. I., Chekova, S. V., Tsarkova, A. S., Golubev, Y. V., Negrebetsky, V. V., 620 Dolgushin, S. A., Shalaev, P. V., Shlykov, D., Melnik, O. A., Shipunova, V. O., ... Sarkisyan, K. S. (2020). Plants with genetically encoded autoluminescence. 621 622 Nature Biotechnology, 38(8), 944–946. https://doi.org/10.1038/s41587-020-0500-9 623 624 Mott, G. A., Desveaux, D., & Guttman, D. S. (2018). A High-Sensitivity, Microtiter-Based

Plate Assay for Plant Pattern-Triggered Immunity. Molecular Plant-Microbe 625 626 Interactions, 31(5), 499–504. https://doi.org/10.1094/MPMI-11-17-0279-TA Navarro, L., Zipfel, C., Rowland, O., Keller, I., Robatzek, S., Boller, T., & Jones, J. D. G. 627 628 (2004). The transcriptional innate immune response to flg22. Interplay and 629 overlap with Avr gene-dependent defense responses and bacterial pathogenesis. 630 *Plant Physiology*, 135(2), 1113–1128. https://doi.org/10.1104/pp.103.036749 Ngou, B. P. M., Ahn, H.-K., Ding, P., & Jones, J. D. G. (2021). Mutual potentiation of 631 632 plant immunity by cell-surface and intracellular receptors. *Nature*, 592(7852), 633 110–115. https://doi.org/10.1038/s41586-021-03315-7 634 Nguyen, H. P., Chakravarthy, S., Velásquez, A. C., McLane, H. L., Zeng, L., Nakayashiki, H., Park, D.-H., Collmer, A., & Martin, G. B. (2010). Methods to 635 636 study PAMP-triggered immunity using tomato and Nicotiana benthamiana. 637 Molecular Plant-Microbe Interactions, 23(8), 991–999. 638 https://doi.org/10.1094/MPMI-23-8-0991 639 Pruitt, R. N., Locci, F., Wanke, F., Zhang, L., Saile, S. C., Joe, A., Karelina, D., Hua, C., 640 Fröhlich, K., Wan, W.-L., Hu, M., Rao, S., Stolze, S. C., Harzen, A., Gust, A. A., 641 Harter, K., Joosten, M. H. A. J., Thomma, B. P. H. J., Zhou, J.-M., ... Nürnberger, 642 T. (2021). The EDS1–PAD4–ADR1 node mediates Arabidopsis pattern-triggered 643 immunity. Nature, 598(7881), 495-499. https://doi.org/10.1038/s41586-021-644 03829-0 Qi, J., Wang, J., Gong, Z., & Zhou, J.-M. (2017). Apoplastic ROS signaling in plant 645 646 immunity. Current Opinion in Plant Biology, 38, 92–100. 647 https://doi.org/10.1016/j.pbi.2017.04.022

Sahdev, S., Saini, S., Tiwari, P., Saxena, S., & Singh Saini, K. (2007). Amplification of 648 649 GC-rich genes by following a combination strategy of primer design, enhancers 650 and modified PCR cycle conditions. Molecular and Cellular Probes, 21(4), 303-651 307. https://doi.org/10.1016/j.mcp.2007.03.004 652 Schmelz, E. A., Carroll, M. J., LeClere, S., Phipps, S. M., Meredith, J., Chourey, P. S., 653 Alborn, H. T., & Teal, P. E. A. (2006). Fragments of ATP synthase mediate plant 654 perception of insect attack. Proceedings of the National Academy of Sciences, 103(23), 8894–8899. https://doi.org/10.1073/pnas.0602328103 655 656 Segretin, M. E., Pais, M., Franceschetti, M., Chaparro-Garcia, A., Bos, J. I. B., Banfield, 657 M. J., & Kamoun, S. (2014). Single Amino Acid Mutations in the Potato Immune Receptor R3a Expand Response to Phytophthora Effectors. Molecular Plant-658 659 Microbe Interactions, 27(7), 624–637. https://doi.org/10.1094/MPMI-02-14-0040-660 R 661 Stamatakis, A. (2014). RAxML version 8: A tool for phylogenetic analysis and post-662 analysis of large phylogenies. Bioinformatics, 30(9), 1312–1313. https://doi.org/10.1093/bioinformatics/btu033 663 664 Steinbrenner, A. D. (2020). The evolving landscape of cell surface pattern recognition across plant immune networks. Current Opinion in Plant Biology, 56, 135–146. 665 666 https://doi.org/10.1016/j.pbi.2020.05.001 667 Steinbrenner, A. D., Goritschnig, S., & Staskawicz, B. J. (2015). Recognition and Activation Domains Contribute to Allele-Specific Responses of an Arabidopsis 668 669 NLR Receptor to an Oomycete Effector Protein. PLOS Pathogens, 11(2), e1004665. https://doi.org/10.1371/journal.ppat.1004665 670

Steinbrenner, A. D., Muñoz-Amatriaín, M., Chaparro, A. F., Aguilar-Venegas, J. M., Lo, 671 672 S., Okuda, S., Glauser, G., Dongiovanni, J., Shi, D., Hall, M., Crubaugh, D., Holton, N., Zipfel, C., Abagyan, R., Turlings, T. C. J., Close, T. J., Huffaker, A., & 673 674 Schmelz, E. A. (2020). A receptor-like protein mediates plant immune responses 675 to herbivore-associated molecular patterns. Proceedings of the National Academy of Sciences, 117(49), 31510-31518. 676 677 https://doi.org/10.1073/pnas.2018415117 678 Thorne, N., Inglese, J., & Auld, D. S. (2010). Illuminating insights into firefly luciferase 679 and other bioluminescent reporters used in chemical biology. Chemistry & 680 Biology, 17(6), 646–657. https://doi.org/10.1016/j.chembiol.2010.05.012 681 Toyota, M., Spencer, D., Sawai-Toyota, S., Jiaqi, W., Zhang, T., Koo, A. J., Howe, G. 682 A., & Gilroy, S. (2018). Glutamate triggers long-distance, calcium-based plant 683 defense signaling. Science, 361(6407), 1112-1115. 684 https://doi.org/10.1126/science.aat7744 685 van der Burgh, A. M., Postma, J., Robatzek, S., & Joosten, M. H. A. J. (2019). Kinase activity of SOBIR1 and BAK1 is required for immune signalling. Molecular Plant 686 Pathology, 20(3), 410–422. https://doi.org/10.1111/mpp.12767 687 688 Van Leeuwen, W., Hagendoorn, M. J. M., Ruttink, T., Van Poecke, R., Van Der Plas, L. 689 H. W., & Van Der Krol, A. R. (2000). The use of the luciferase reporter system for in planta gene expression studies. Plant Molecular Biology Reporter, 18(2), 143-690 691 144. https://doi.org/10.1007/BF02824024 692 Wang, P.-H., Kumar, S., Zeng, J., McEwan, R., Wright, T. R., & Gupta, M. (2020). 693 Transcription Terminator-Mediated Enhancement in Transgene Expression in

Maize: Preponderance of the AUGAAU Motif Overlapping With Poly(A) Signals. 694 695 Frontiers in Plant Science, 11. 696 https://www.frontiersin.org/article/10.3389/fpls.2020.570778 697 Wang, Y., Li, X., Fan, B., Zhu, C., & Chen, Z. (2021). Regulation and Function of 698 Defense-Related Callose Deposition in Plants. *International Journal of Molecular* 699 Sciences, 22(5), 2393. https://doi.org/10.3390/ijms22052393 700 Zhang, L., Hua, C., Pruitt, R. N., Qin, S., Wang, L., Albert, I., Albert, M., van Kan, J. A. 701 L., & Nürnberger, T. (2021). Distinct immune sensor systems for fungal 702 endopolygalacturonases in closely related Brassicaceae. Nature Plants, 7(9), 703 1254–1263. https://doi.org/10.1038/s41477-021-00982-2 704 Zhang, L., Kars, I., Essenstam, B., Liebrand, T. W. H., Wagemakers, L., Elberse, J., 705 Tagkalaki, P., Tjoitang, D., Ackerveken, G. van den, & Kan, J. A. L. van. (2014). 706 Fungal Endopolygalacturonases Are Recognized as Microbe-Associated 707 Molecular Patterns by the Arabidopsis Receptor-Like Protein 708 RESPONSIVENESS TO BOTRYTIS POLYGALACTURONASES1. Plant 709 *Physiology*, 164(1), 352–364. https://doi.org/10.1104/pp.113.230698 710 Zhang, Z., Fradin, E., de Jonge, R., van Esse, H. P., Smit, P., Liu, C.-M., & Thomma, B. 711 P. H. J. (2013). Optimized Agroinfiltration and Virus-Induced Gene Silencing to 712 Study Ve1-Mediated Verticillium Resistance in Tobacco. Molecular Plant-Microbe 713 Interactions, 26(2), 182–190. https://doi.org/10.1094/MPMI-06-12-0161-R Zipfel, C., Kunze, G., Chinchilla, D., Caniard, A., Jones, J. D. G., Boller, T., & Felix, G. 714 715 (2006). Perception of the bacterial PAMP EF-Tu by the receptor EFR restricts 716 Agrobacterium-mediated transformation. *Cell*, 125(4), 749–760.

https://doi.org/10.1016/j.cell.2006.03.037

Figure Legends

Figure 1. *Agrobacterium* and In11-induced changes in *N. benthamiana* gene expression. A, Venn diagram displaying number of significantly differentially expressed genes (DEGs) upregulated by *Agrobacterium* relative to mock-treated tissue. B, *Agrobacterium*-downregulated genes. Treatments are labeled as follows: AH, *Agrobacterium* + H2O, AI, *Agrobacterium* + In11, H, Mock infiltrated leaf tissue. See Fig. S1 for treatment details. Top ten genes in both categories with largest log2(fold-change) (FC) are displayed at right. P-value indicates statistical significance with standard Wald test. Adj. P indicates significance after correction for multiple comparisons (Benjamani-Hochberg, BH). C, Candidate genes induced by In11 in the presence of *Agrobacterium*. While only one DEG was observed after BH correction, 9 genes were induced by In11 uncorrected for multiple comparisons (Fig. S1).

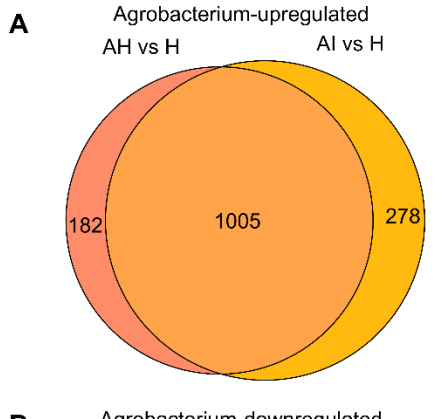
Figure 2. qRT-qPCR validation of candidate marker genes. Boxplots indicate the mean log₂(fold change) between water and ln11 treated tissue (log₂(FC) ln11 vs H₂O) of gene expression from *N. benthamiana* plants expressing either p35s::PvINR or an empty vector (EV) over four biological replicates. Student's t-tests were conducted to determine significance (n.s.: not significant p>.05, *: p<0.05, **: p<0.01, ***: p<0.001).

Figure 3. A *Nicotiana benthamiana LYS1* homolog serves as a marker of inceptin response. A, Leaves were coinfiltrated with *p35s::PvINR* and *pLYS1::LUZ* across the proximal portion of the leaf, and *p35s::PvINR* and *p2xLYS1::LUZ* across the distal portion of the leaf. 48 hours after infiltration, one half of the leaf was infiltrated with sterile water, and the other half was infiltrated with 1 μM In11. Images were obtained 6 hours after peptide treatment, and ASI was quantified in ImageJ. Left, boxplots show the average ASI of three independent biological replicates. Letters represent significantly different means (One-way ANOVA and post-hoc Tukey's HSD tests, p<.05). Right, a representative leaf image of one biological replicate is depicted. B, Leaves were co-infiltrated with *p35s::PvINR* and *p2xLYS1::LUZ* in six distinct regions of the leaf. 48 hours after infiltration each zone was infiltrated with sterile water or a series of In11 concentrations. Imaging and quantification were conducted as in A.

Figure 4. The *p2xLYS1::LUZ* construct acts as a generic reporter for plant pattern recognition receptors. Leaves of *N. benthamiana* plants were coinfiltrated with the *p2xLYS1::LUZ* reporter construct and either A) empty vector, B) *35s::PvINR*, C) *35s::AtEFR*, or D) *35s::AtRLP23* in four distinct regions. 48 hours after infiltration, each

region was infiltrated with either sterile water, 1 μ M In11, 1 μ M elf18, or 1 μ M nlp20 peptide. Images were obtained 6 hours after peptide treatment, and ASI was quantified in ImageJ. Left, boxplots show the average ASI of six independent biological replicates. Letters represent significantly different means (One-way ANOVA and post-hoc Tukey's HSD tests, p<.05). Right, a representative leaf image of one biological replicate is depicted.

Figure 5. SOBIR1 is necessary for activation of luminescence by PvINR. Leaves of *Nicotiana benthamiana sobir1* knockout plants were coinfiltrated with the *pFBP_2xLYS1::LUZ* reporter construct, *p35s::PvINR* and either: empty vector (EV); A) *p35s::PvSOBIR1; or B) p35s::AtSOBIR1* , repeated for three biological replicates. 48 hours after infiltration, each region of interest was infiltrated with either sterile water or 1 μM In11. Images were obtained 6 hours after peptide treatment, and ASI was quantified in ImageJ. Left, boxplots show the average ASI of three independent biological replicates. Letters represent significantly different means (One-way ANOVA and post-hoc Tukey's HSD tests, p<.05). Right, a representative leaf image of one biological replicate is depicted.



		Agro + H ₂ O (AH) vs H ₂ O (H)		
Gene	Niben101 Functional Annotation	log2(FC)	p-value	adj. p
Niben101Scf09186g00006	trypsin proteinase inhibitor precursor [Nicotiana tabacum]	-3.43	9.35E-20	4.39E-17
Niben101Scf01685g12005	Xyloglucan endotransglucosylase/hydrolase protein 9	-2.94	1.44E-14	3.69E-12
Niben101Scf05216g09026	PDZ, K-box, TPR	-1.85	4.07E-14	9.95E-12
Niben101Scf00887g02006	Ornithine decarboxylase	-4.92	1.21E-13	2.80E-11
Niben101Scf11490g00008	Thiamine thiazole synthase	-1.40	9.52E-13	1.86E-10
Niben101Scf07638g01010	Seed storage 2S albumin superfamily protein	-3.06	1.99E-12	3.53E-10
Niben101Scf03404g00007	BnaA06g36820D [Brassica napus]	-2.33	2.74E-12	4.73E-10
Niben101Scf05073g02002	Transcription factor EB	-4.93	3.93E-11	5.43E-09
Niben101Scf10316g01005	carbohydrate binding protein, putative [Ricinus communis]	-2.66	7.62E-11	1.01E-08
Niben101Scf05782g00010	Oxygen-evolving enhancer protein 2-1, chloroplastic	-1.68	9.77E-11	1.25E-08

В	Agrobacterium-downregulated							
	AH vs h	H Alv	s H					
	226	506	343					

С

		Agro + H ₂ O (AH) vs H ₂ O (H)		
Gene	Niben101 Functional Annotation	log2(FC)	p-value	adj. p
Niben101Scf01084g03003	No annotation (BLASTX: NbSAR8.2d)	7.82	5.14E-123	1.21E-118
Niben101Scf03385g02011	Plant basic secretory protein (BSP) protein	7.82	2.39E-110	2.80E-106
Niben101Scf35444g00004	Glutathione S-transferase U8	6.84	3.57E-85	2.79E-81
Niben101Scf02819g00005	Early nodulin-like protein 1	7.42	2.47E-69	1.45E-65
Niben101Scf02041g00002	Chitinase 8	4.66	7.48E-67	3.51E-63
Niben101Scf10735g00016	Major pollen allergen Bet v 1-M/N	5.17	9.52E-58	3.73E-54
Niben101Scf02410g00002	Chitinase 9	7.30	1.92E-47	6.43E-44
Niben101Scf05404g09001	Glutathione S-transferase U8	8.25	7.11E-44	2.09E-40
Niben101Scf02171g00007	chitinase [Zea mays subsp. parviglumis]	7.25	1.20E-42	3.14E-39
Niben101Scf02203g05002	3-hydroxy-3-methylglutaryl-coenzyme A reductase	5.10	2.00E-41	4.70E-38

		Agro + In11 (Al) vs Agro + H2O (AH)			Agro + H ₂ O (AH) vs H ₂ O (H)			
Gene	Niben101 Functional Annotation	log2(FC)	p-value	adj. p	log2(FC)	p-value	adj. p	
Niben101Scf08566g08014	Peroxidase N1	2.05	2.97E-09	1.08E-04	2.85	1.45E-12	2.70E-10	
Niben101Scf04592g00020	BURP domain-containing protein 3	2.40	1.00E-04	1.00E+00	5.16	9.53E-05	2.43E-03	
Niben101Scf02513g05010	Peroxidase N1	1.36	4.79E-04	1.00E+00	4.74	1.99E-20	9.95E-18	
Niben101Scf09387g01003	Seed storage 2S albumin superfamily protein	1.22	3.18E-03	1.00E+00	5.35	3.66E-15	1.02E-12	
Niben101Scf03444g02004	BAG family molecular chaperone regulator 2	1.32	4.13E-03	1.00E+00	2.16	5.03E-04	9.11E-03	
Niben101Scf02411g01001	Peroxidase 4	1.02	6.73E-03	1.00E+00	5.01	3.08E-08	2.36E-06	
Niben101Scf06684g03003	Acidic endochitinase	2.13	2.21E-02	1.00E+00	3.29	2.73E-02	1.77E-01	
Niben101Scf01534g02007	Annexin D4	1.02	4.42E-02	1.00E+00	1.69	2.38E-03	3.05E-02	
Niben101Scf04652g00027	Unknown protein	1.53	4.80E-02	1.00E+00	2.64	3.71E-02	2.18E-01	

Figure 1. *Agrobacterium* and In11-induced changes in *N. benthamiana* gene expression. A, Venn diagram displaying number of significantly differentially expressed genes (DEGs) upregulated by *Agrobacterium* relative to mock-treated tissue. B, *Agrobacterium*-downregulated genes. Treatments are labeled as follows: AH, *Agrobacterium* + H2O, AI, *Agrobacterium* + In11, H, Mock infiltrated leaf tissue. See Fig. S1 for treatment details. Top ten genes in both categories with largest log2(fold-change) (FC) are displayed at right. P-value indicates statistical significance with standard Wald test. Adj. P indicates significance after correction for multiple comparisons (Benjamini-Hochberg, BH). C, Candidate genes induced by In11 in the presence of *Agrobacterium*. While only one DEG was observed after BH correction, 9 genes were induced by In11 uncorrected for multiple comparisons (Fig. S1).

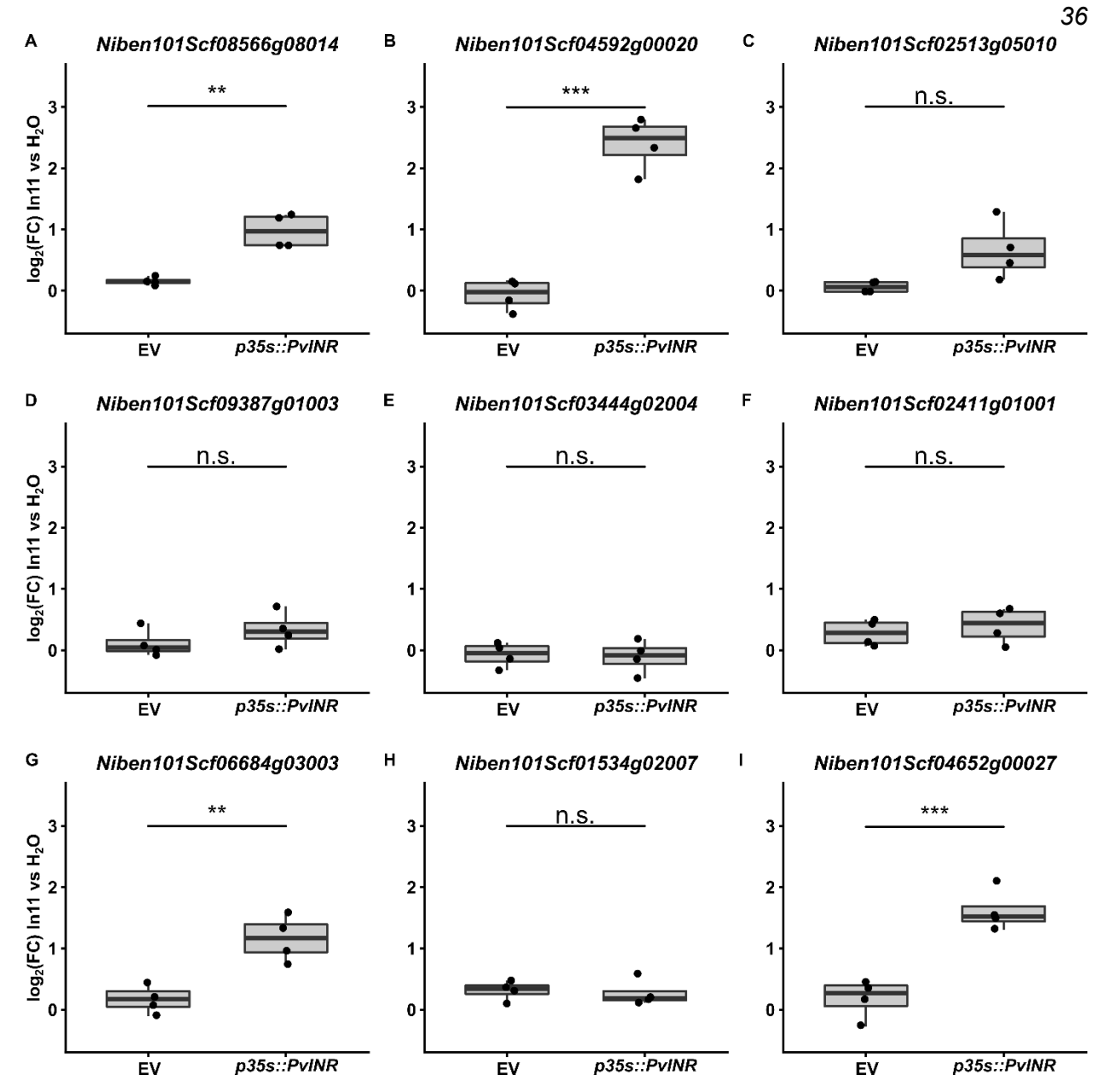
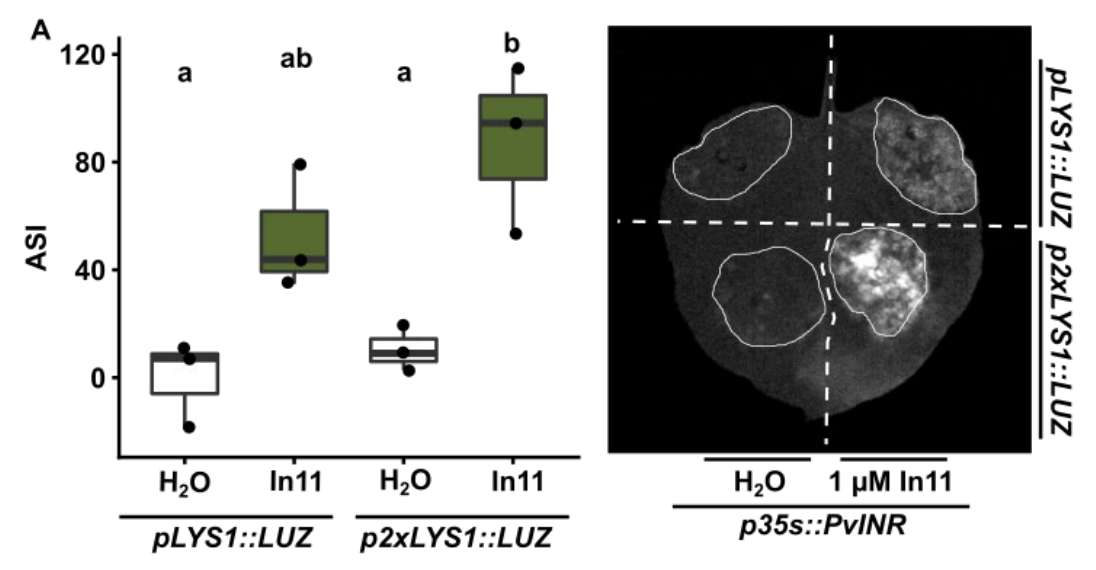


Figure 2. qRT-qPCR validation of candidate marker genes. Boxplots indicate the mean $log_2(fold\ change)$ between water and In11 treated tissue $(log_2(FC)\ In11\ vs\ H_2O)$ of gene expression from *N. benthamiana* plants expressing either p35s::PvINR or an empty vector (EV) over four biological replicates. Student's t-tests were conducted to determine significance (n.s.: not significant p>.05, *: p<0.05, **: p<0.01, ***: p<0.001).



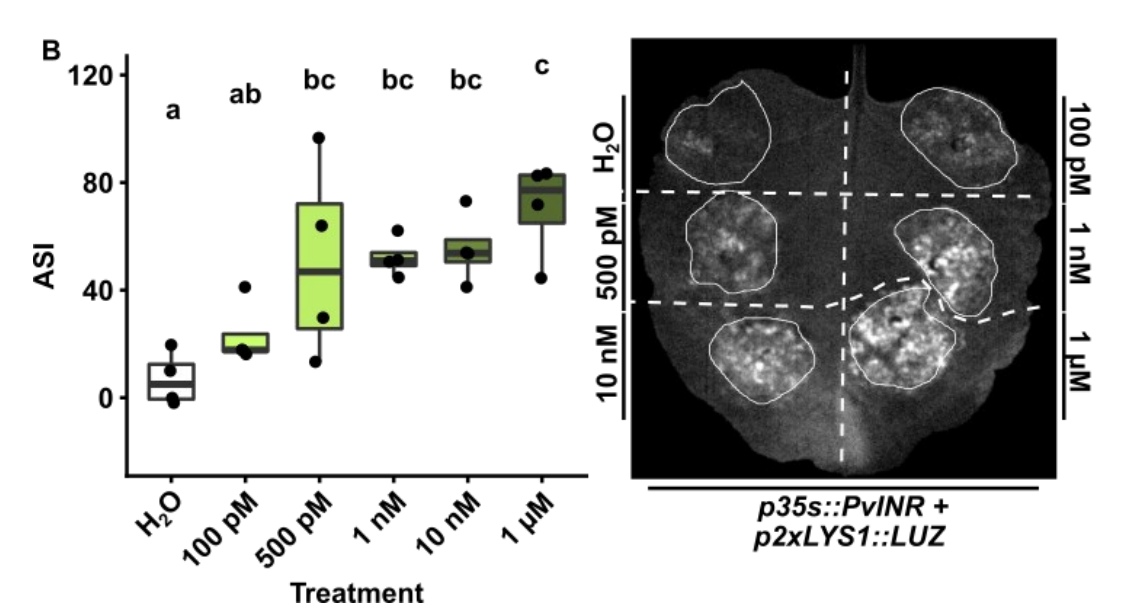


Figure 3. A Nicotiana benthamiana LYS1 homolog serves as a marker of inceptin response. A, Leaves were coinfiltrated with *p35s::PvINR* and *pLYS1::LUZ* across the proximal portion of the leaf, and *p35s::PvINR* and *p2xLYS1::LUZ* across the distal portion of the leaf. 48 hours after infiltration, one half of the leaf was infiltrated with sterile water, and the other half was infiltrated with 1 μM In11. Images were obtained 6 hours after peptide treatment, and ASI was quantified in ImageJ. Left, boxplots show the average ASI of three independent biological replicates. Letters represent significantly different means (One-way ANOVA and post-hoc Tukey's HSD tests, p<.05). Right, a representative leaf image of one biological replicate is depicted. B, Leaves were co-infiltrated with *p35s::PvINR* and *p2xLYS1::LUZ* in six distinct regions of the leaf. 48 hours after infiltration each zone was infiltrated with sterile water or a series of In11 concentrations. Imaging and quantification were conducted as in A.

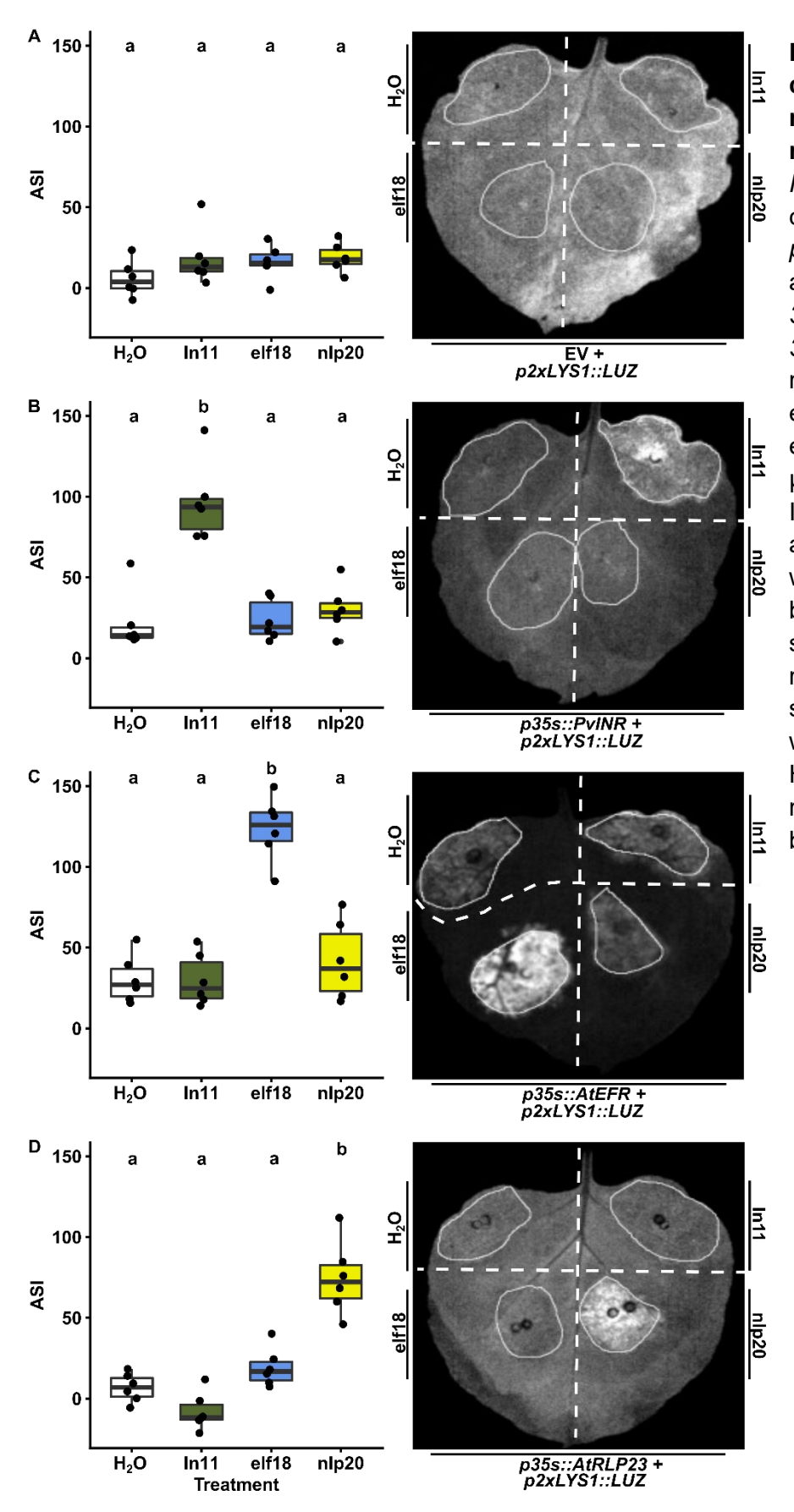


Figure 4. The p2xLYS1::LUZ construct acts as a generic reporter for plant pattern recognition receptors. Leaves of N. benthamiana plants were coinfiltrated with the p2xLYS1::LUZ reporter construct and either A) empty vector, B) 35s::PvINR, C) 35s::AtEFR, or D) 35s::AtRLP23 in four distinct regions. 48 hours after infiltration, each region was infiltrated with either sterile water, 1 µM In11, 1 μM elf18, or 1 μM nlp20 peptide. Images were obtained 6 hours after peptide treatment, and ASI was quantified in ImageJ. Left, boxplots show the average ASI of six independent biological replicates. Letters represent significantly different means (Oneway ANOVA and post-hoc Tukey's HSD tests, p<.05). Right, a representative leaf image of one biological replicate is depicted.

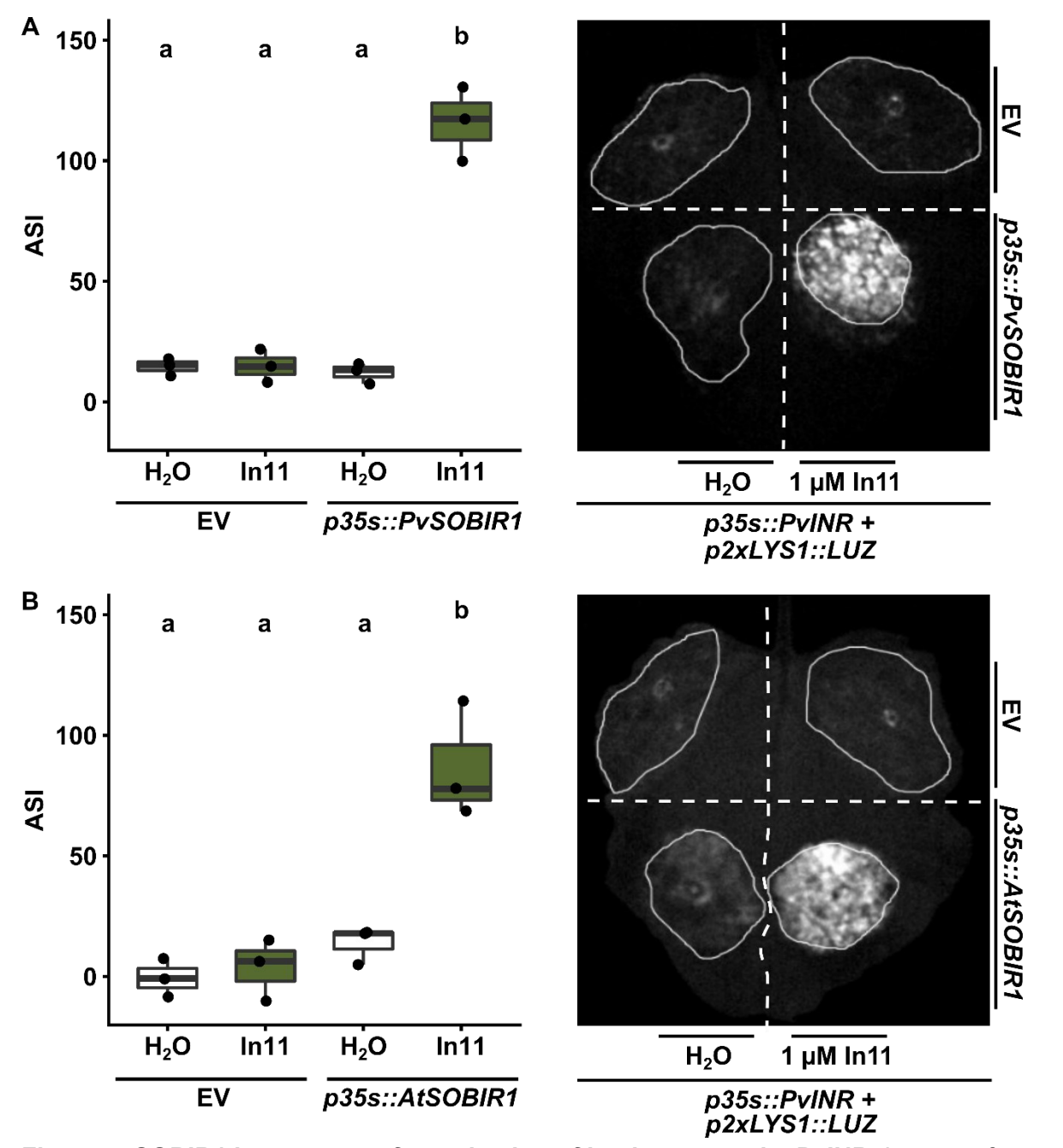


Figure 5. SOBIR1 is necessary for activation of luminescence by PvINR. Leaves of *Nicotiana benthamiana sobir1* knockout plants were coinfiltrated with the *pFBP_2xLYS1::LUZ* reporter construct, *p35s::PvINR* and either: empty vector (EV); A) *p35s::PvSOBIR1; or B*) *p35s::AtSOBIR1*, repeated for three biological replicates. 48 hours after infiltration, each region of interest was infiltrated with either sterile water or 1 μM In11. Images were obtained 6 hours after peptide treatment, and ASI was quantified in ImageJ. Left, boxplots show the average ASI of three independent biological replicates. Letters represent significantly different means (Oneway ANOVA and post-hoc Tukey's HSD tests, p<.05). Right, a representative leaf image of one biological replicate is depicted.